

High Gain Antenna System Deployment Mechanism Integration, Characterization, and Lessons Learned

Fil Parong*, Blair Russell**, Walter Garcen**, Chris Rose⁺, Chris Johnson**, and Craig Huber**

Abstract

The integration and deployment testing of the High Gain Antenna System for the Global Precipitation Measurement mission is summarized. The HGAS deployment mechanism is described. The gravity negation system configuration and its influence on vertical, ground-based, deployment tests are presented with test data and model predictions. A focus is made on the late discovery and resolution of a potentially mission degrading deployment interference condition. The interaction of the flight deployment mechanism, gravity negation mechanism, and use of dynamic modeling is described and lessons learned presented.

Introduction

During testing and integration of the High Gain Antenna System (HGAS) to the core Global Precipitation Measurement (GPM) spacecraft, a potential deployment hardware interference issue was discovered. A release mechanism firing order change along with trimming a structurally critical bracket was chosen as a solution to increase clearance. A dynamic software model was built that predicted the worst-case, on-orbit deployment path of the HGAS. The model showed that the firing order change and the material removed from the HGAS hardware provided sufficient clearance margin for a successful deployment.

GPM Mission Overview

The GPM core spacecraft will carry a high gain antenna system to provide command and control communications as well as a science data downlink through the Tracking and Data Relay Satellite System (TDRSS). The GPM mission is an international network of satellites that will provide the next-generation global observations of rain and snow. The GPM mission deploys a “core” satellite carrying an advanced radar/radiometer system to measure precipitation from space and serves as a reference standard to unify precipitation measurements from a constellation of research and operational satellites. The GPM team, initiated by National Aeronautic and Space Administration (NASA) and the Japan Aerospace Exploration Agency (JAXA), comprises a consortium of international space agencies. The GPM Core Spacecraft is qualified and scheduled to launch in late February 2014. [<http://pmm.nasa.gov/GPM>]

HGAS Configuration and Design

The assembled HGAS system, shown in Figure 1, has a mass of 95 kg (210 lbm), including 24 kg (52 lbm) for the gimballed antenna assembly. When stowed, it occupies a roughly 2.8 m x 1.0 m x 0.9 m (110 in x 39 in x 35 in) volume, and deploys 3.6 m (140 in) from its base.

For antenna pointing, the GPM HGAS employs a two-axis gimbal configuration. Due to field-of-view requirements and packaging limitations, the HGAS boom assembly consists of two boom sections with shoulder and elbow hinges that contain coaxial deployment springs and dampers. A synchronization (sync) cable provides redundancy for the dampers and deployment springs, allowing for system deployment in the event of a spring or damper failure. The sync cable also helps maintain the ratio of the two hinge angles to approximately 2:1, as the elbow and shoulder hinges open 180 and 90 degrees respectively during deployment.

* National Aeronautics and Space Administration Goddard Space Flight Center

** Stinger Ghaffarian Technologies Incorporated

⁺ Vantage Systems Incorporated

HGAS contains five mechanisms: three Launch Restraint Mechanisms (LRM's), a Lower Boom Assembly (LBA), and the gimbal assembly. The upper boom connects the LBA to the gimbal assembly as shown in Figure 1. The entire HGAS assembly and associated mechanism are supported on an all-aluminum honeycomb plate. The LRMs and hinge line designs were developed from heritage Solar Dynamics Observatory hardware.

Launch Restraint Mechanism

The HGAS uses three LRMs (known as the A, B, and C devices) to restrain the upper boom and the gimbal assembly to the mounting plate prior to deployment. Each LRM is composed of a latch rod, securing the upper boom or gimbal assembly to two spring loaded jaws. Each jaw is attached to a non-explosive actuator (NEA). After firing, the NEAs release the latch rods allowing the system to deploy. As designed, LRM C releases first, followed four seconds later by the LRMs A and B simultaneously. Deployment commences once all LRMs are released. Kick-off springs at LRM B and LRM C assist in separating the HGAS assembly from the LRMs.

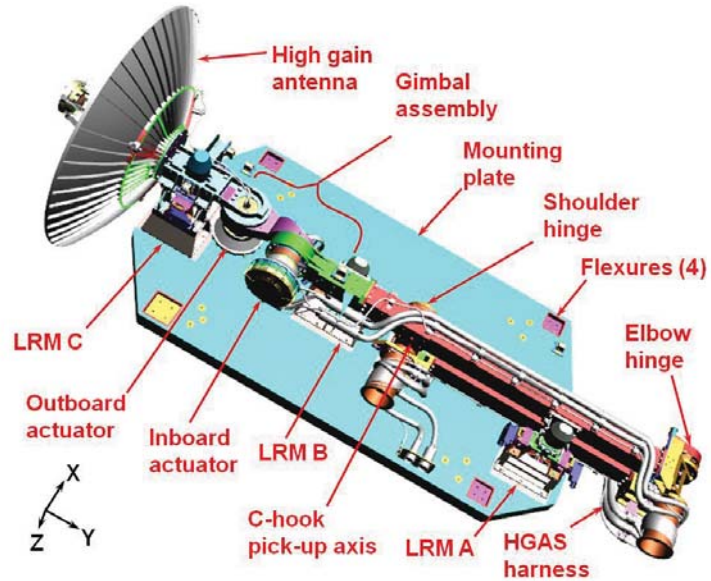


Figure 1: HGAS Layout

Lower Boom Assembly

The LBA, shown in Figure 2, is made up of the two deployment hinges; the elbow hinge and shoulder hinge, connected via a 0.77 m (30 in) long lower boom. Each hinge incorporates a constant torque deployment spring, a viscous fluid damper, and a potentiometer (for hinge angle telemetry).

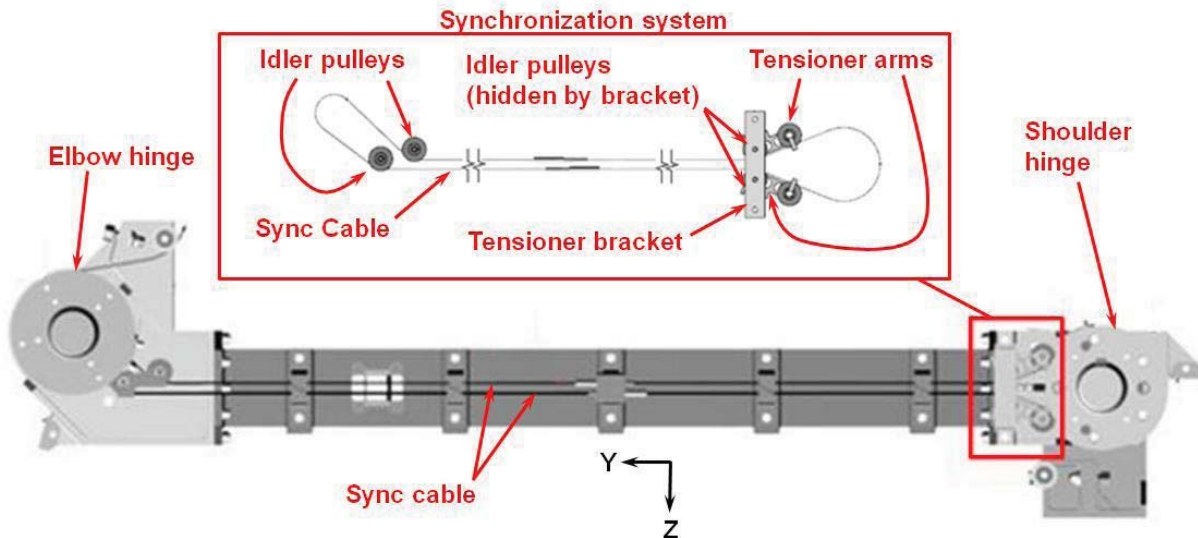


Figure 2: Lower Boom Assembly, Key Components

Gimbal Assembly

The two-axis gimbal assembly consists of two actuators using a stepper motor and harmonic drive gear reduction in each axis. Both axes can rotate $\pm 90^\circ$ in 0.0075° increments. The gimbal is commanded using pitch (local X) and yaw (local Y) axis design orientation made up of a lower actuator bracket that connects to the upper boom, a middle linkage bracket, and an antenna bracket mounted to the High Gain Antenna (HGA). The gimbal assembly provides the HGA with the capability to access multiple TDRSS satellite communication links continuously throughout the GPM mission.

Hinge Spring and Damper Development and Sizing

Resistance torque testing of the hinge system was performed to determine the minimum torque required to deploy the system. A design deployment spring torque of 11.3 N-m (100 in-lbf) at both the elbow and shoulder hinges was selected, leaving adequate torque margin at each hinge.

The HGAS elbow hinge uses the same size and type viscous fluid damper as was already selected for GPM's solar array deployment system. Taking this known damping rate and design deployment spring torques as givens, along with the intent for the HGAS to deploy at a 2:1 ratio, the shoulder hinge's required damping rate was calculated. Since the damping varies strongly with temperature, both damper temperatures are actively controlled with external heaters to $30.0^\circ\text{C} \pm 2.0^\circ\text{C}$ ($86^\circ\text{F} \pm 3.6^\circ\text{F}$) for flight.

Synchronization System

A synchronization cable system was added to provide redundancy and control of the deployment path to the mechanism. The elbow and shoulder hinges are connected via a stainless steel sync cable, which helps to maintain the 2:1 intended hinge angle ratio. The pulleys connected to the hinges are sized for this 2:1 ratio. The sync cable's tension is maintained with a spring-loaded tensioning system that applies additional tension via two spring loaded tensioner arms. This tensioning system was sized primarily for thermal gradient cases, as there can be a worst case 65°C (149°F) gradient along the lower boom. Since the ratio between elbow and shoulder hinges was designed as 2:1, a metric called the *elbow delta angle* (Δ) was defined as follows:

$$\Delta = \text{elbow angle} - 2 \times \text{shoulder angle} \quad (1)$$

A positive Δ indicates the elbow is leading the shoulder during deployment. A negative Δ indicates the elbow is trailing the shoulder. *The design intent, and thus the expected value of Δ , is zero or negligibly off zero throughout the deployment.*

Gravity Negation System

The gravity negation (g-negation) system enables a vertical deployment of the HGAS in a 1-g environment. Such deployments are required to characterize and qualify the HGAS system prior to flight. The HGAS deployment system qualification included three spacecraft integrated deployments; immediately after initial integration to spacecraft, after thermal vacuum testing (T-Vac), and after vibration testing. Due to packaging constraints, accommodations for other deployable systems, and configuration requirements for operational tests on the ground, the HGAS g-negation system was required to enable vertical deployments. Other options such as deploying perpendicular to gravity (horizontally) on a low friction surface were not compatible with GPM program requirements.

The g-negation scheme utilizes three discreet counter mass elements sized to g-negate individual sections of the HGAS. The system is comprised of a four-bar mechanism, a concentrated mass/moment arm, and a counter mass connected by cables and pulleys through an overhead gantry. The g-negation system, attached to the HGAS, is sketched in Figure 3. Ground Support Equipment (GSE) is drawn in bold lines, while the HGAS flight hardware is drawn in thin lines. Shown partially deployed, heavy solid arrows indicate the direction of motion of the moving parts of the g-negation system.

Counter Torque Assembly

The Counter Torque Assembly (CTA) imparts a torque to the HGAS shoulder hinge line. The intent of the CTA is to negate the effects of gravity on the lower boom of the HGAS assembly as it rotates through its 90 degree deployment. The torque is produced by an adjustable mass mounted to a moment arm. The torque is transmitted to the shoulder hinge line via a four bar linkage. The magnitude of the torque decreases as the moment arm rotates through 90° from horizontal to vertical. In the absence of the deployable portion of HGAS above the elbow hinge, the CTA would negate the force of gravity on the lower boom throughout its rotation, assuming no applied torques from the harness or deployment springs.

Elbow Counter Mass

The elbow counter mass balances the upper boom and gimbal assembly about the C-hook pickup axis. It consists of a mass block and a 'U' shaped bracket; the mass of each may be adjusted. Were the lower boom absent, the upper boom and gimbal/HGA assembly would be torque balanced about the C-hook pickup axis, assuming no applied torques from the harness or deployment springs. The addition of the elbow counter mass to the upper boom requires that this mass is also negated by the C-hook counter mass.

Gantry/C-Hook Counter Mass

The gantry/C-hook counter mass assembly is intended to negate the effects of gravity on the mass of the upper boom, gimbal assembly, and the elbow counter mass. The system consists of a modified commercial off-the-shelf gantry, a 'C' shaped link (C-hook), a counter mass and a cable/pulley system. The gantry, in its configuration to support spacecraft integrated HGAS deployments, measured 7.6 m (25 ft) tall by 6.1 m (20 ft) wide and 3.6 m (12 ft) deep. It includes a substantial amount of ballast mass at its base to meet stability requirements. The total mass of the upper boom, gimbal/HGA assembly, and elbow counter mass is g-negated by the C-Hook counter mass.

Assuming a 2:1 ratio between the shoulder and elbow hinge angles is properly maintained and the HGAS mounting plate is parallel to the ground, the C-hook pick up axis on the upper boom should stay directly over the shoulder hinge axis. This allows a vertical cable to provide the g-negation for the upper boom/gimbal assembly through the C-hook pickup axis. The C-hook link allows the load path to go around the antenna dish when the HGAS is deployed. The g-negation system, with HGAS integrated to the spacecraft, is shown in Figure 4.

Stow/Deployment Bias

Ideally the system will exactly negate the effects of gravity on the HGAS for ground tests. As this is not feasible, the g-negation system will either hinder or aid in the deployment of the system. In order to confidently qualify the deployment system, it is important that the g-negation system does not assist deployment. To be conservative in ground testing, the system should be tuned to slightly hinder deployment or bias the system toward the stowed configuration. This is referred to as stow bias.

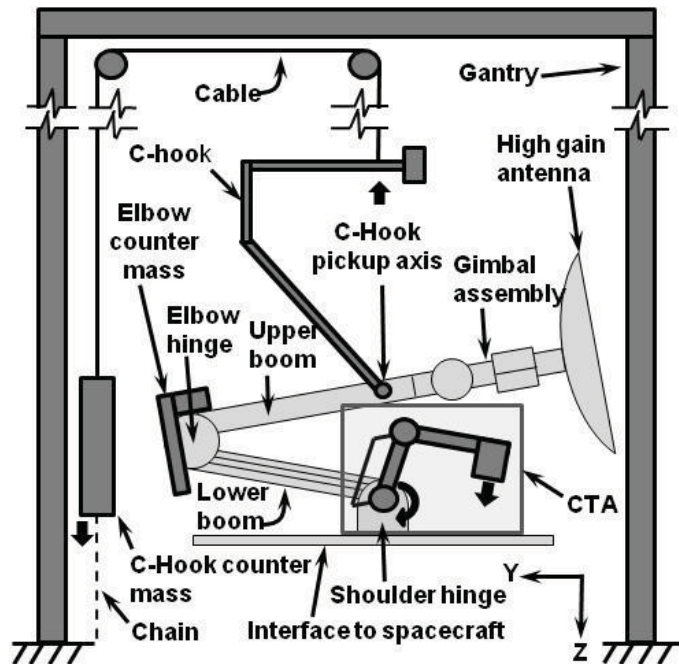


Figure 3: HGAS G-Negation System

Stow bias is the load or torque applied by the g-negation system that retards system deployment compared to a “perfectly” gravity negated state. A deployment bias would be a load or torque that assists deployment.

The starting point for calculating the masses of the g-negation system’s three elements was the development of an accounting/moment balance spreadsheet. This spreadsheet tracked mass and moment arm for the lower and upper booms separately as well as the three g-negation elements. The mass and moment arm data was comprised of actual measured inertia, CAD-based inertial information, and engineering estimates. This data was used to sum the torques and masses and determine what counter mass was needed for each of the three g-negation elements. This g-negation configuration is specific to the flight hardware configuration for which it was determined.

During HGAS subsystem integration, the g-negation was verified by removing the deployment springs (harness was not present at this time) and observing system motion. Small changes to the mass configuration were made to fine tune the system.

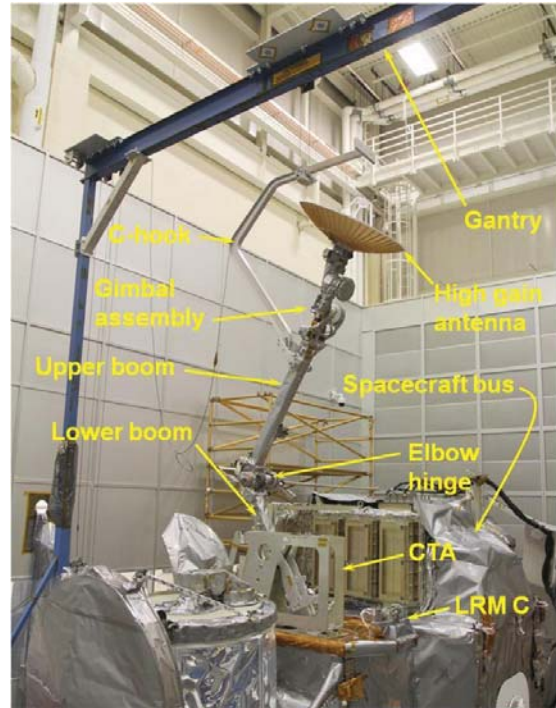


Figure 4: HGAS during g-negated deployment testing, integrated to GPM spacecraft

Any mass changes to the deployable section of the HGAS impacts the g-negation configuration. The addition of T-Vac test instrumentation, then vibration test instrumentation, and later removal of this hardware required changes to the g-negation mass configuration. These changes were determined analytically, with the balance spreadsheet, as it was no longer an option to remove the harness and deployment springs to verify the stow/deployment bias. This is a key limitation in ground testing.

Deployment Instrumentation

As part of the ground support equipment, instrumentation was developed to document deployment tests. Inclinometers were added to the lower and upper booms to track their angles during deployment. Loads in the g-negation system were recorded via two load cells on either end of the C-hook cable assembly. The load cells were used primarily to ensure the stow/deployment bias did not change appreciably during deployment. Data from the inclinometers was more useful. From inclinometer data, the deployment rates for the shoulder and elbow hinge can be determined, as well as the elbow delta angle (Δ). This data is shown in Figure 5.

Subtleties of G-negation System

There were several subtleties discovered during the early trials. While the gantry cable and pulley system is intended to only apply a vertical force to g-negate the upper boom/ gimbal assembly, any tendency of the C-hook pickup axis to move laterally from a vertical path will be met with a centering reaction at the C-hook pickup axis (see Figure 9). This reaction is the horizontal component of the tension in the cable and increases as the cable angle deviates from vertical. This centering effect also increases as the HGAS deploys as cable length shortens and angle increases. For a deviation of 76 mm (3 in), the horizontal centering force would be on the order of 10 N (3 lb) for the fully deployed system. If HGAS deploys along its designed path this force is negligible.

Another subtlety discovered was the effect of cable length/mass switching sides of the g-negation cable/pulley system. As the system deployed, cable length on C-hook end of the cable/pulley system would shorten, while cable length on the C-hook counter mass end of the system would lengthen by an equal amount. The C-hook pickup axis moves vertically 1.9 m (75 in) during deployment. This effectively increased the counter mass on the C-hook counter mass side of the cable and thus decreased the amount of stow bias from the g-negation system by approximately 0.75 Kg (1.65 lb) at the end of deployment. This feature was corrected by the addition of a length of chain (with the same linear density as the cable) to the C-hook counter mass. The chain was hung from the C-hook counter mass to a collection pan on the floor. As the length of cable shortened on the C-hook side of the cable/pulley system, the same length of chain piled up in the collection pan on the floor, balancing the effect.

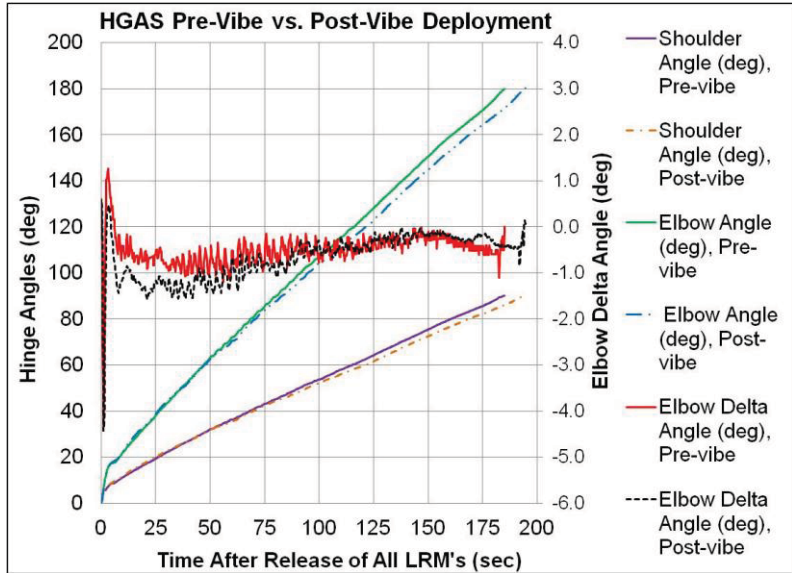


Figure 5: Deployment Data for HGAS Qualification

Baseline (Flight-like) Dynamic Model

During the course of GPM HGAS manufacture and integration, a dynamic HGAS computer model was developed using MSC ADAMS to aid in predicting on-orbit deployment path and deployment time. Later, the model was enhanced by adding ground deployment GSE to simulate g-negated ground deployments.

The ADAMS model was very much a “living document”. It was first built with nominal values for spring torques, dampers, masses, etc. The model was continually updated as more accurate information of various flight components became available. Eventually, the model migrated towards representing the flight configuration in high fidelity with the exception of certain unknowns such as hinge friction coefficients and in-situ harness torques. Key features of the model are detailed below:

- *Hinge Deployment Spring Torque:* The deployment spring torque at both hinges used the torque vs. angle data gathered for the serialized flight springs during sub-component testing. While the springs were intended to be constant torque springs, the torque isn't truly constant and varies as a function of angle.
- *Variable Damping Coefficients:* The fluid hinge dampers have damping coefficients that are a function of angular velocity and temperature. In addition, the damping varies unit to unit. Damping performance at various temperatures and angular velocities was measured in the serialized flight units. Damping coefficient vs. angular velocity curves, at various temperatures, were generated based on that test data and incorporated into the ADAMS model.
- *Damper Deadband:* The dampers have a deadband, which is a span of a few degrees of rotation where there is no damping. Once the damper rotates past the deadband angle, damping suddenly comes into play. Some of the deadband is due to mechanical play in the damper attachment to the hinge while the rest is internal to the damper. Below the deadband angle, damping was simply

switched off in the ADAMS model. Note that the deadband of the elbow damper and that of the shoulder damper were not the same.

- *Sync Cable Compliance:* Based on bench test data of a flight-like cable and tensioner, the compliance of the sync cable was incorporated into the ADAMS model. It was added as a non-linear spring function applied to the elbow hinge that was the Δ function previously discussed. A positive Δ indicates the elbow is leading the shoulder and an internal resistive torque would be applied to the elbow by the model. A negative Δ indicates the elbow is trailing the shoulder and an internal assistive torque would be applied to the elbow. Larger magnitude Δ 's would result in greater internal elbow torque magnitudes applied by the spring-like model. Whenever the Δ was zero, the hinges are synchronized and no internal torque would be applied to the elbow by the model. An example of the Δ is plotted as elbow angle delta in Figure 5. A mathematical construct known as a "coupler" in ADAMS was used to tie the elbow hinge to the shoulder hinge with a 2:1 ratio. The compliance torque function was serially applied at the elbow end of this coupler to simulate the compliance in the sync cable system.
- *Use of Measured Masses:* Actual measured masses were used for the booms, gimbal, and antenna. The mass used for HGAS harnesses were from the flight spares. Blanket and instrumentation masses are approximated. Center of gravity (CG) locations were not known for the flight subassemblies so the ADAMS model CG locations were matched to that of the CAD model.
- *Variable Harness Torque:* The HGAS harness torque as a function of angle imparted at each hinge was measured on the qualification unit at various temperatures. That data was incorporated into the ADAMS model.
- *Flexible Body Structures:* Both booms, the lower actuator bracket, middle linkage bracket, and the antenna bracket were modeled as flexible elements. ADAMS uses Timoshenko beam relations for such structures.
- *LRM Spring Energy:* The LRM retractor springs were assumed to be 90% efficient in terms of the energy they would deliver to the retractors when fired. The design value for the preload and stiffness was used for each retractor spring.
- *Friction:* Frictions in hinges, deployment springs, dampers, and cable pulleys were not load or rotation angle dependent. For these frictions, maximum expected vendor values were used.
- *Kick-off Springs at LRMs:* The kick-off springs at LRM B and LRM C are included in the model as preloaded linear springs.

The ADAMS model could be run either as an on-orbit model or as a ground test model ("g-negated"). Starting with the g-negated model, the ADAMS model could be easily converted to the on-orbit model by turning off gravity and disabling all the g-negating components of the model and vice-versa.

The model was calibrated using the results of g-negated ground tests. As the model evolved and more g-negated tests were performed, the model's calibration was iteratively tuned. The target for calibration was deployment time and damper deadband performance. The adjustments made to the model during calibration were to the hinge deadband angles and g-negation system stow bias.

On plots of hinge angles vs. time for ground tests, one can pick out the deadband angle of the particular dampers as there is an inflection point in the slope of the curve. The slope changes sign as the dampers activate outside their deadband angle. These characteristic inflection points are noted in Figure 6. Once the deadband angle was picked off the graph, that angle could be incorporated into the model. The model simulation would then be repeated to ensure that the inflection points occurred at approximately the same angle as seen in the test data.

As it could not be actually measured, the stow bias was the least certain value in the ADAMS model. To finalize calibration of the model, the stow bias was iterated until the latch time of both hinges closely matched the latching (i.e. fully deployed) times in the most current g-negated tests. The hinges would not latch at the exact same time due to compliance in the sync cable, allowing the small Δ angle between the two hinges.

The final calibration to the ADAMS model was done using the post T-Vac, g-negated, deployment data. The hinge angles of the post T-vac test and the corresponding calibrated ADAMS model predictions are compared in Figure 6. The 3 N (0.7 lbf) of stow bias used to calibrate the model compares favorably to the 2 to 4.4 N (0.5 to 1.0 lbf) stow bias estimated by the test engineers prior to the test. This calibrated model became the baseline ADAMS model. This baseline model, run as a “on-orbit” (i.e. zero gravity and g-negation system model elements disabled) would be used to predict on-orbit performance of the flight configuration HGAS.

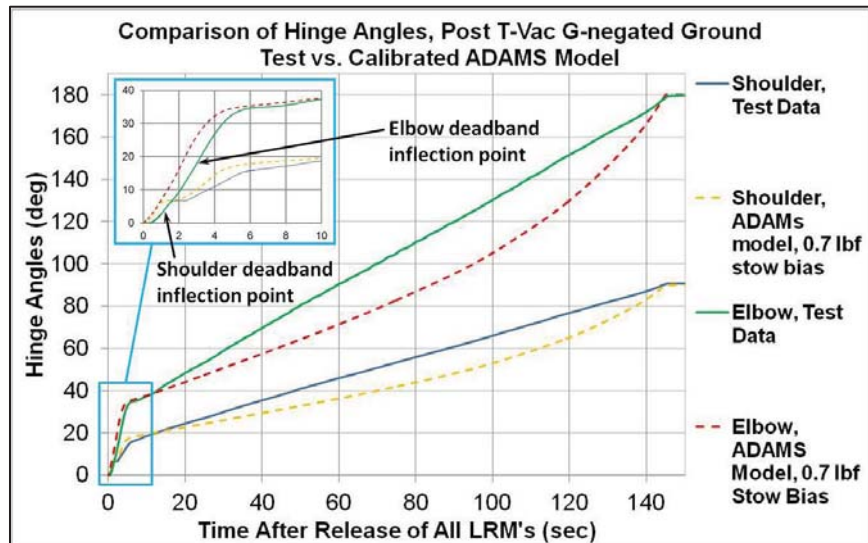


Figure 6: Calibrated ADAMS Model Predicted Hinge Angles Compared to G-Negated Test Values

Potential Deployment Interference

After the HGAS subsystem was integrated to the spacecraft, a potential deployment interference issue between the outboard actuator of the gimbal assembly and LRM C was discovered (see Figure 7). The potential interference was discovered while doing an analysis run with the HGAS ADAMS model for another purpose (i.e. non-baseline), not to check for interferences between the gimbal assembly and LRM C.

The predicted interference was verified with a run of the baseline ADAMS model. It was noticed that the HGAS gimbal assembly penetrated into the rectangular solid representing LRM C (again, see Figure 7). While constraint (e.g. hinges) locations are based off the CAD model and thus accurately located in the HGAS ADAMS model, not all the geometry is accurately portrayed, so the ADAMS model, by itself, cannot be relied on to check for interferences.

The ADAMS model results for elbow and shoulder hinge angles were inserted into the CAD model to check for interferences. The CAD model also predicted an interference of the outboard actuator with LRM C (see Figure 8). In the event this interference led to a failed deployment by jamming the outboard actuator against LRM C, the core spacecraft would lose its high bandwidth communication ability and would have to rely on a much slower data rate. This would delay completing or possibly compromise the completion of mission objectives.

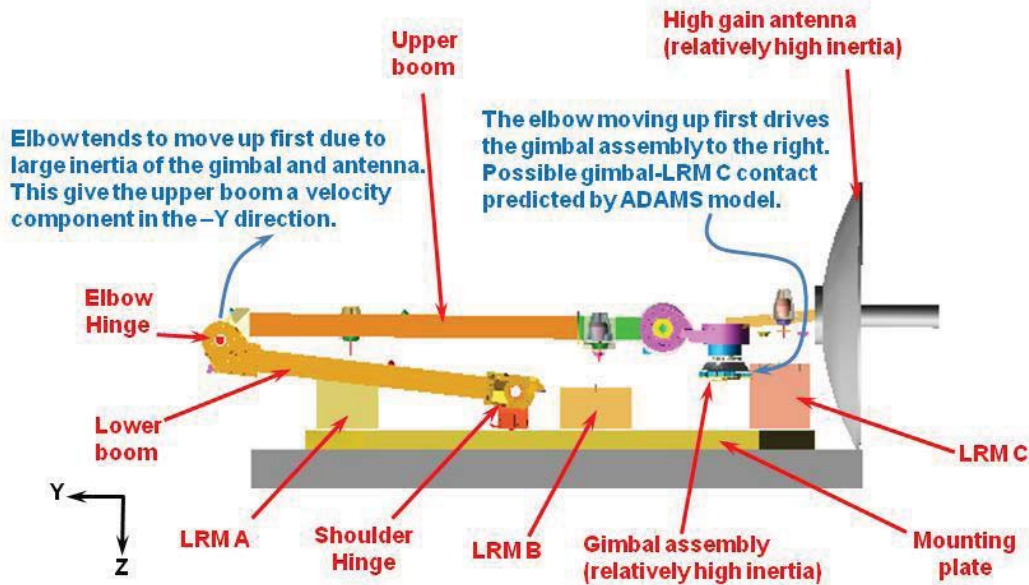


Figure 7: Potential Impact of Gimbal Section with LRM C (image from ADAMS model)

This discovery led to close examination of the HGAS deployable and the following revelation: The potential interference issue is rooted in a fundamental trait of the design. It is *kinematically indeterminate* with no set deployment path. The ramifications of this were not understood during the design phase or even early in the testing phase, as it was assumed that the sync cable would keep the elbow and shoulder hinges' rotation locked in a tight 2:1 ratio. In reality, compliance in the synchronization cable allows some independent rotation of the elbow hinge relative to the shoulder hinge. The ratio tends towards 2:1, but isn't necessarily 2:1. This kinematically indeterminate system resulting from the sync cable compliance allows the following to influence the HGAS deployment path:

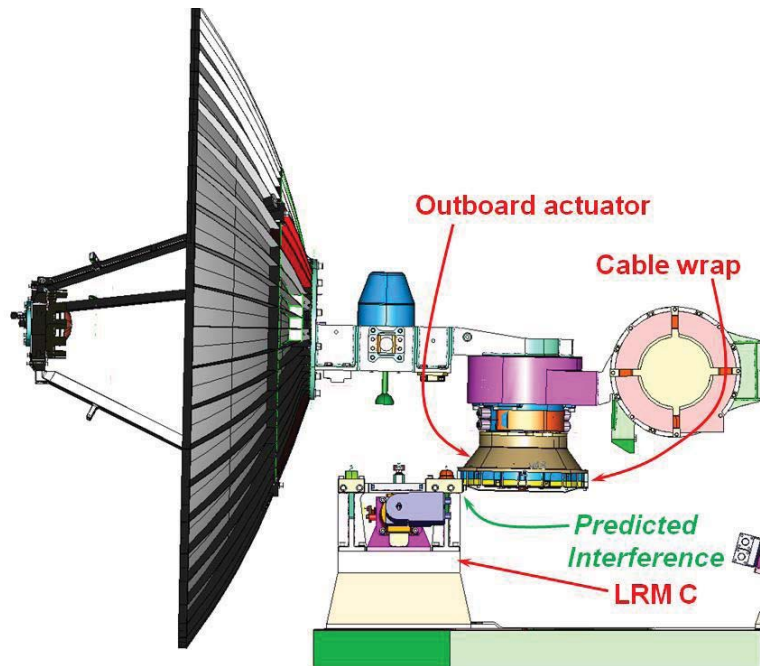


Figure 8: CAD Model Used to Verify Interference Predicted by Baseline Adams Model

- **Gimbal/Antenna Inertia:** The relatively large gimbal assembly and antenna inertia resists movement and thus the elbow end tends to lift off the deck first. Due to the geometry of the boom, this lifting of the elbow drives the gimbal assembly towards the non-deploying LRM C structure on the HGAS deck (see Figure 7).

- *Stored Energy in LRMS:* Impact energy from the firing of the launch restraint mechanisms and the force of the kick-off springs at each LRM can compound the issue. The LRM release order plays a significant role in the deployment path.
- *G-negation System Design:* G-negation system biases can influence the deployment path, masking the potential for on-orbit (i.e. zero-g) deployed interference. See Figure 9. During ground testing, contact was unlikely to be observed because the g-negation system biases the deployment path towards the intended design path (i.e. tends to center HGAS and assist the sync cable).

To check the validity of the baseline dynamics model and CAD predictions of the interference condition with LRM C, a hardware range of motion system check was performed. This check was done as early as the flight hardware was available. The HGAS was g-negated and all system preload was removed. Using careful hand manipulation, the system was moved through potential ranges of motion. From this study, it was verified that contact between deploying system members and non-deploying hardware could indeed occur. The principle point of contact was the outboard actuator with the +X, +Y corner at the top (-Z) edge of the spherical constraint tower assembly of the LRM C. The interference resolution was well under way at the time the issue was verified on the flight hardware.

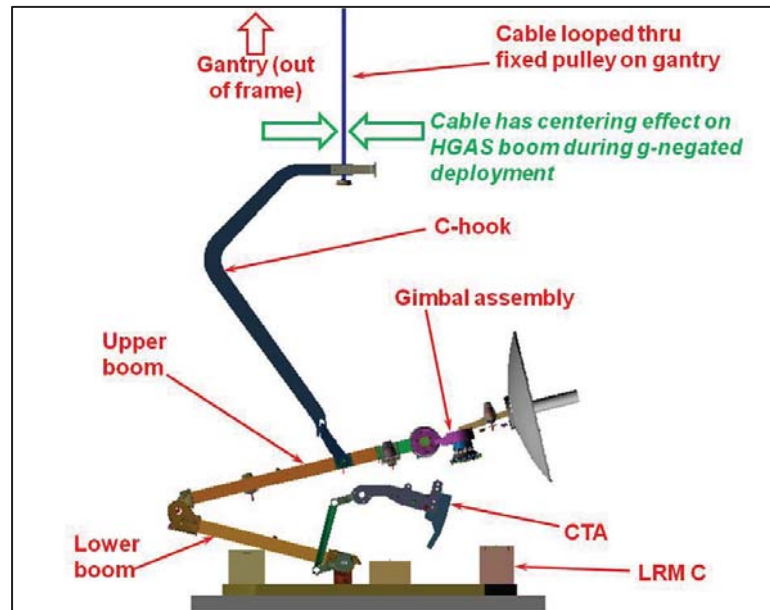


Figure 9: Gantry Cable tends to Center HGAS During G-negated Ground Deployment Tests (image from ADAMS model)

Interference-Biased ADAMS Model

Because the HGAS is kinematically indeterminate, whether there was sufficient clearance for the flight deployment path could not be determined without use of dynamic motion analysis. This analysis must include appropriate conservatism to ensure sufficient margin on clearance and a good design.

The calibrated baseline ADAMS model was key in developing a solution for the potential interference issue as the flight hardware was unavailable for detailed in situ subsystem study and testing. The HGAS was already integrated on the GPM spacecraft and the tight spacecraft integration and test schedule severely limited the team's access to the hardware.

To use the dynamic HGAS ADAMS model to investigate potential solutions, appropriate conservatism was applied to the various parameters in the model. The type of conservatism applied to a dynamic model depends on the result one intends to study. For instance, with hinge deployment spring torque, if one wanted to be conservative with hinge "end of travel" impact velocity, you would use the high end of the deployment spring torque tolerance. If one wanted to be conservative on deployment time (i.e. the longest time) one would use the low end of deployment hinge spring torque tolerance, as lower torques translate to slower deployment speeds. When comparing and investigating the potential solutions of the

interference issue, the metric used was the *minimum clearance between the gimbal assembly and LRM C* at any moment in time during the deployment.

Out of many dozens, the team identified 26 model parameters or factors that could have significant effect on this clearance. Using the baseline “on-orbit” model as the starting point, all these factors were biased to reasonable extremes that *would minimize* clearance. For most of the 26 factors, those extremes were given by known tolerances. For the remaining factors, engineering judgment was used. This altered baseline model would become our *reasonable worst-case interference-biased model*, referred to hereafter as the “worst case” model. The team decided that a design solution was achieved if our ADAMS modeling efforts showed a minimum clearance of 6.4 mm (0.25 inches) between hard parts when running the on-orbit version of this worst case model.

This approach was considered robust because it was highly improbable that all 26 factors would be simultaneously biased towards minimum clearance in the actual flight hardware. Also, the HGAS ADAMS model had historically showed good correlation to the g-negated tests, especially in the first 15 degrees of shoulder hinge rotation.

As mentioned previously, the fidelity of the g-negation system to confidently test for interference of the gimbal with LRM C was insufficient due to the centering effect the gantry cable has on the HGAS during ground testing. Therefore, this worst case ADAMS model represented the best tool available to vet this issue.

There is insufficient space to describe the kinematic role of all 26 factors in this worst case model, but the three examples below demonstrate the typical methodologies used for biasing factors:

- *Shoulder Deployment Spring Torque:* A higher value of the shoulder spring torque would lift the elbow off the HGAS deck more quickly and thus further increase the interference of the gimbal assembly with LRM C (see Figure 7). Since the model was already using spring torques measured off the actual flight shoulder spring, variances in those torques would be driven by the error in the torque transducer used to measure the springs. The claimed accuracy of said transducer was $\pm 4\%$. Thus, it is possible for the measured torque to be up to 4% lower than the actual value. To be conservative on clearance in the worst case model, the torque vs. hinge angle curve for the shoulder deployment spring was multiplied by 1.04 (+4%)
- *Elbow Deployment Spring Torque:* Conversely, a lower value of elbow spring torque would result in a slower lifting of the gimbal assembly off LRM C and thus reduce clearance/increase interference. As with the shoulder, the model was already using spring torques measured off the actual flight elbow spring. The same transducer was used to measure the flight elbow spring torque. In this case, we wanted to minimize the spring torque in the worst case model to achieve the appropriate conservatism, so the elbow spring torque function was multiplied by 0.96 (-4%).
- *Elbow Damper Temperature:* Viscous dampers are used at each of the hinges. Thus the damping coefficients are functions of temperature. Decreasing temperature increases the damping. Heaters on the dampers control their temperatures to $30\text{ }^{\circ}\text{C} \pm 2\text{ }^{\circ}\text{C}$ ($86\text{ }^{\circ}\text{F} \pm 3.6\text{ }^{\circ}\text{F}$) As previously noted, hindering elbow rotation decreases clearance, thus the elbow damper temperature was set to $28\text{ }^{\circ}\text{C}$ ($82.4\text{ }^{\circ}\text{F}$) and the damping coefficient vs. hinge angular velocity curve in the model reflected the resulting increase in damping.

Both the baseline ADAMS model and the worst case model were used to determine the path forward. Due to time constraints, the early runs that illuminated the potential issue were used to guide potential hardware changes while the analysis team decided on the final conservative values for the aforementioned 26 critical factors of the worst case model. During this period, the baseline model was

used to study the effect of proposed hardware and flight operation changes. Model hinge angle results were incorporated into the CAD model to check actual clearances.

Issue Resolution

The solution to the interference issue was a combination of adjusting the firing/release order of the three launch restraint mechanisms (C then A/B became A/B then C) and trimming of non-deploying portions of the LRM C hardware to increase dynamic clearance.

Reversing the LRM release order improved the originally predicted 1.0 mm (0.04 inches) interference to 12 mm (0.46 inches) of clearance in the baseline model. With C firing first, followed by A/B four seconds later (i.e. the original firing order), the ADAMS model predicted that the retractor impact and kick-off spring energy at C was mostly absorbed by the x-axis gimbal actuator, contributing nothing to separating the HGAS from the surrounding structure. With the firing order reversed (A/B followed by C four seconds later), the model predicted that the firing of A and B does not change the hinge geometry significantly as the structure is still held down at C. But when LRM C is finally fired, the retractor and kick-off spring energy are efficiently used to rotate the HGAS away from the other structures about the elbow hinge axis. This operational change was implemented in the on-orbit deployment commands through the GPM engineering change request system. It was successfully utilized on all subsequent ground deployment tests.

Although the baseline model predicted 12 mm (0.46 inches) of clearance, the criteria for a successful design solution was 6.35 mm (0.25 inches) of predicted minimum clearance from the on-orbit version of the worst case model. A quick model run, assuming only one of the 26 factors biased towards interference (i.e. retractors transferring no impact energy to the booms), brought the predicted clearance back down to 4.8 mm (0.19 inches). A similar run with the worst case model was not done as the clearance was already below the target minimum. This necessitated trimming LRM C's tower assembly.

Figure 10 provides an overview of LRM C and the related constraint components. The spherical tower assembly of LRM C was nearest to the outboard actuator and was the location of predicted interference.

The most direct solution was to remove the corner material of each component in the tower assembly. At this stage of GPM testing and integration, HGAS had completed subsystem environmental test verification and had been delivered and integrated to the flight spacecraft. Thus modifying the test verified hardware could create a programmatic risk by nullifying the test verification. However, spacecraft environmental testing had not yet begun and it was deemed that modification of constraint components would not violate previous verification so long as load path and contact stress were not compromised. Workmanship for reassembly would be verified through spacecraft level environmental testing. Removal of tower component corner material up, to but shy of, the constraint contact region

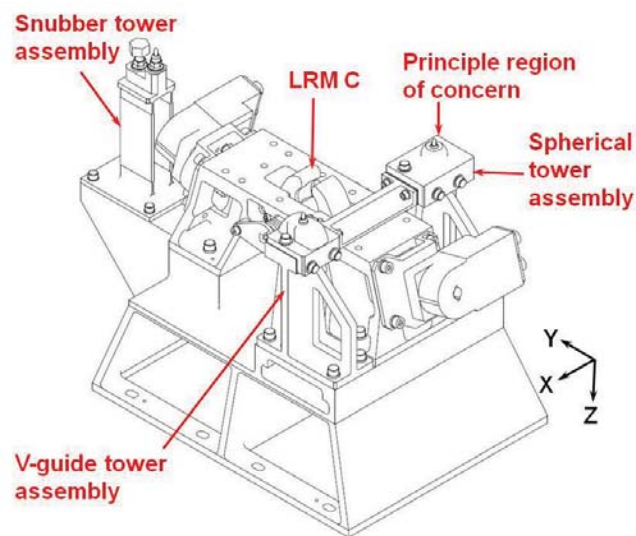


Figure 10: LRM-C Constraint Component Assembly

meant the removal of two tower assembly fasteners. Sub-assembly finite element analysis was performed with this change in place and yielded an acceptable margin.

Modification of the constraint tower assembly components required tower assembly removal from HGAS. As the tower was pinned to the HGAS deck and already qualified, the decision was made to modify the installed components rather than flight spares. Positional relocation was not then a concern. Figure 11 illustrates the component modifications performed to ensure the desired deployment clearances.

Once removed from HGAS, the tower assembly was delivered to metrology for coordinate measuring machine documentation of tower assembly height and critical feature positions. In doing so, proper fitment of the modified and reassembled tower assembly could be verified.

The tower assembly was then disassembled and the individual components were modified via CNC machining. Piece part metrology verification was performed prior and after component modification.

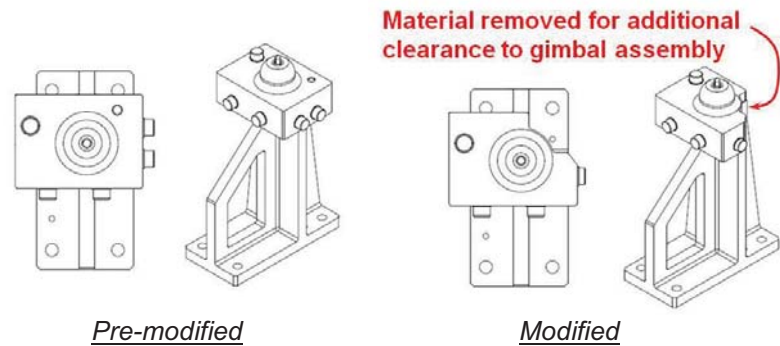


Figure 11: LRM-C Spherical Tower Assembly

Tower reassembly then occurred. The now modified spherical tower assembly itself received metrology verification. With spherical tower assembly modification complete, it was installed to its previously pinned HGAS location and its interface to the stowed HGAS constraints was verified by measurement.

The element of the gimbal assembly which could interfere with the constraint tower during deployment was the outboard gimbal cable wrap (see Figure 8). The cable wrap hardware was enveloped in a multi-layer thermal blanket. To maximize clearance at the potential location of contact, a section of blanket was removed from the gimbal harness wrap and replaced with a single layer of vapor deposited aluminum Kapton™ tape. Modification of the blanket was performed in situ.

With the trimmed hardware, the baseline simulations now indicated a 19 mm (0.76 in) clearance. Since the approval metric was based on using the worst case model, another simulation was run, which predicted a clearance of 12 mm (0.48 inches). This exceeds the minimum clearance of 6.35 mm (0.25 inches) by almost a factor of two. The design was acceptable.

The hand manipulation motion studies were repeated and clearance verified. Spacecraft level deployments and environmental testing followed. With respect to the component modifications performed, spacecraft environment testing was complete with the successful post-environmental test deployment. Functional and workmanship verification was achieved.

Lessons Learned

The late discovery and resolution of a potentially mission degrading interference issue has yielded several pertinent lessons.

The compliance in cable synchronization systems in articulating multi-boom systems may allow significant non-kinematic behavior. A particular deployment travel path cannot be assumed. Designing to this assumption led to the development of a g-negation system that biases the deployment to the intended path. This can mask interference or other issues that ground testing is intended to uncover. In the present

case, this was discovered during the integration and test phase of the spacecraft development, long after the design phase was complete.

Assuming the deployment path also led to giving up some clearance during the design phase in order to accommodate other packaging needs. If the kinematic indeterminate nature of this deployable was understood and appreciated at the time, clearance would not have been sacrificed. For such a system, more clearance should be kept in reserve. Although not always possible due to space constraints, a good “rule of thumb” is to avoid having deploying hardware below the break plane between the LRMs and the deploying hardware so that clearance increases monotonically during deployment.

The parallel development of a dynamic computer model of this complex deployable and its g-negation system proved indispensable. It allowed detection of the interference condition and informed the solution to the issue. It saved cost and schedule as much of the work was conducted offline while the spacecraft continued its integration and test program. As the HGAS subsystem hardware was integrated, the fidelity of the model was increased. As ground tests were performed, the model was calibrated. In the end, it was a very valuable tool that allowed the investigation and understanding of a complex deployable in a way that would have been difficult without it.

Acknowledgements

The authors would like to acknowledge the all team members that were involved in the conception, development and delivery of HGAS to GPM as well as those that assisted in the issue resolution and editing of this paper. Specific acknowledgements to: Chris Strickland (Product Development Lead), Tim Pike (Designer/Engineer), Chris Mathews (Mechanical Technician), Danny Grove (Designer), Andrew Lea (Test Engineer), Bryon Stepp (Stress Analyst), John Tota (Quality Assurance), Wahid Zewari (Engineer), Minh Phan (Chief Engineer), Rodger Farley (Senior Staff Engineer), and Mark McGinnis (Reviewer).